Evidence of Quadrupole and Octupole Deformations in math xmlns="http://www.w3.org/1998/Math/MathML" display="inline">mrow>mmultiscripts>mrow>mi>Zr/mi>/mrow>mprescripts>/mprescripts>none>/none>mrow>mn>96/mn>/mrow>/mmultiscripts>mo>+/mo>mmultiscripts>mrow>mi>Zr/mi>/mrow>mprescripts>/mprescripts>none>/none>mrow>mn>96/mn>/mrow>/mmultiscripts>/mrow>/math> and math xmlns="http://www.w3.org/1998/Math/MathML" display="inline">mrow>mmultiscripts>mrow>mi>Ru/mi>/mrow>mprescripts>/mprescripts>none>/none>mrow>mn>96/mn>/mrow>/mmultiscripts>mo>+/mo>mmultiscripts>mrow>mi>Ru/mi>/mrow>mprescripts>/mprescripts>none>/none>mrow>mn>96/mn>/mrow>/mmultiscripts>/mrow>/math> Collisions at Ultrarelativistic Energies

Chunjian Zhang and Jiangyong Jia

Phys. Rev. Lett. **128**, 022301 — Published 11 January 2022

DOI: 10.1103/PhysRevLett.128.022301

Evidence of quadrupole and octupole deformations in ^{96}Zr+^{96}Zr and ^{96}Ru+^{96}Ru collisions at ultra-relativistic energies

Chunjian Zhang[1] and Jiangyong Jia[1,2,*]

[1] *Department of Chemistry, Stony Brook University, Stony Brook, NY 11794, USA*
[2] *Physics Department, Brookhaven National Laboratory, Upton, NY 11976, USA*

In the hydrodynamic model description of heavy ion collisions, the elliptic flow v_2 and triangular flow v_3 are sensitive to the quadrupole deformation β_2 and octupole deformation β_3 of the colliding nuclei. The relations between v_n and β_n have recently been clarified and were found to follow a simple parametric form. The STAR Collaboration have just published precision v_n data from isobaric ^{96}Ru+^{96}Ru and ^{96}Zr+^{96}Zr collisions, where they observe large differences in central collisions $v_{2,\mathrm{Ru}} > v_{2,\mathrm{Zr}}$ and $v_{3,\mathrm{Ru}} < v_{3,\mathrm{Zr}}$. Using a transport model simulation, we show that these orderings are a natural consequence of $\beta_{2,\mathrm{Ru}} \gg \beta_{2,\mathrm{Zr}}$ and $\beta_{3,\mathrm{Ru}} \ll \beta_{3,\mathrm{Zr}}$. We reproduce the centrality dependence of the v_2 ratio qualitatively and v_3 ratio quantitatively, and extract values of β_2 and β_3 that are consistent with those measured at low energy nuclear structure experiments. STAR data provide the first direct evidence of strong octupole correlations in the ground state of ^{96}Zr in heavy ion collisions. Our analysis demonstrates that flow measurements in high-energy heavy ion collisions, especially using isobaric systems, are a new precision tool to study nuclear structure physics.

PACS numbers: 25.75.Gz, 25.75.Ld, 25.75.-1

Most atomic nuclei present intrinsic deformed shapes, characterized notably by quadrupole, octupole and hexadecapole components [1, 2]. Experimental evidences for nuclear deformation are primarily extracted from spectroscopic measurements and models of reduced transition probability between low-lying rotational states, which involves nuclear experiments with energy per nucleon less than few 10 MeVs. Recently, the prospects of probing the nuclear deformation at much higher beam energy, energy per nucleon exceeding hundreds of GeVs, by taking advantage of the responses of hydrodynamic collective flow of the final state particles to the shape and sizes of the initial state, have been discussed [3–13], and several experimental evidences have been observed [14–18].

Nuclear deformation is often described by a nucleon density in a deformed Woods-Saxon form:

$$\rho(r,\theta,\phi) = \frac{\rho_0}{1+e^{[r-R(\theta,\phi)]/a}},$$
$$R(\theta,\phi) = R_0\left(1+\beta_2 Y_2^0+\beta_3 Y_3^0+\beta_4 Y_4^0\right), \qquad (1)$$

where the nuclear surface $R(\theta,\phi)$ includes only the most relevant axial symmetric quadrupole, octupole and hexadecapole deformations [19].

It is straightforward to see why dynamics of heavy-ion collisions is sensitive to nuclear deformation. These high-energy collisions deposit a large amount of energy in the overlap region, forming a hot and dense quark-gluon plasma (QGP) [20], whose initial shape in the transverse plane is sensitive to the nuclear deformation. This initial shape is characterized via eccentricities $\varepsilon_n = |\int r^n e^{in\phi} e(r,\phi) r dr d\phi / \int r^n e(r,\phi) r dr d\phi|$, estimated from the energy density $e(r,\phi)$ in the overlap. Driven by the pressure gradient forces and subsequent hydrodynamic collective expansion, the initial ε_n are transferred into azimuthal anisotropy of final state hadrons [21], dominated by an elliptic and an triangular modulation of particle distribution, $dN/d\phi \propto 1+2v_2\cos 2(\phi-\Psi_2)+2v_3\cos 3(\phi-\Psi_3)$. The v_n coefficients reflect hydrodynamic response of the QGP to ε_n, and follow an approximate linear relation $v_n = k_n\varepsilon_n$ for events in fixed centrality [22, 23]. In collisions of spherical nuclei, ε_2 mainly reflects the elliptic shape of the overlap controlled by the impact parameter, while non-zero ε_3 arises from random fluctuations of nucleons. The presence of non-zero β_n enhances ε_n, and consequently the values of v_n, which on general ground follow a simple quadratic form [24] for $n = 2$ and 3.

$$\varepsilon_n^2 = a_n' + \sum_{m,k=2}^{4} b'_{n;mk}\beta_m\beta_k, \quad v_n^2 = a_n + \sum_{m,k=2}^{4} b_{n;mk}\beta_m\beta_k, \qquad (2)$$

where ε_n^2 and v_n^2 are mean-square values calculated for events in a narrow centrality. The a_n' and a_n are values for collisions of spherical nuclei, which are strong functions of system size and centrality. In contrast, the coefficients b' and b are expected to be nearly independent of system size [12, 24]. This is because deformations change the distribution of nucleons in the entire nucleus, the coefficients in a give centrality depend mainly on the alignment two nuclei and centrality, not the system size.

All the b' and b terms are not equally important. In fact in the ultra-central collisions (UCC), model studies show that only one deformation term is important [12],

$$\varepsilon_n^2 = a_n' + b_n'\beta_n^2, \qquad v_n^2 = a_n + b_n\beta_n^2. \qquad (3)$$

These simple relations provide a powerful data-driven method to constrain the β_2 and β_3 by comparing collisions of two species with similar sizes, see Refs. [10–12] for details. The most straightforward scenario is to consider collisions of two isobaric systems $X+X$ and $Y+Y$ with the same mass number, therefore having the same

coefficients in Eq. 3. In this case, these ratios have a particularly simple expression,

$$\frac{\varepsilon_{n,Y}^2}{\varepsilon_{n,X}^2} = 1 + \frac{b_n'}{a_n'}(\beta_{n,Y}^2 - \beta_{n,X}^2)/(1 + \frac{b_n'}{a_n'}\beta_{n,X}^2) \approx 1 + \frac{b_n'}{a_n'}(\beta_{n,Y}^2 - \beta_{n,X}^2)\,, \quad (4)$$

$$\frac{v_{n,Y}^2}{v_{n,X}^2} = 1 + \frac{b_n}{a_n}(\beta_{n,Y}^2 - \beta_{n,X}^2)/(1 + \frac{b_n}{a_n}\beta_{n,X}^2) \approx 1 + \frac{b_n}{a_n}(\beta_{n,Y}^2 - \beta_{n,X}^2)\,. \quad (5)$$

The relative ordering of v_n in the two systems is a direct reflection of the ordering of their β_n values [10]. Besides, in the UCC region, the values of a_n' and a_n are smallest and the influence of deformations is largest.

In this Letter, we apply this idea to the recent isobar $^{96}_{40}$Zr+$^{96}_{40}$Zr and $^{96}_{44}$Ru+$^{96}_{44}$Ru collision [25], and make predictions on ratios of v_n from the known values of β_2 and β_3 from nuclear structure measurements, as given in Table I. Assuming the same β_n for neutrons and protons and a uniform charge distribution out to the distance $R(\theta,\phi)$, the β_n values are obtained from the measured reduced electric transition probability $B(En)\uparrow$ via the standard formula [26],

$$\beta_2 = \frac{4\pi}{3ZR_0^2}\sqrt{\frac{B(E2)\uparrow}{\mathrm{e}^2}}\,,\ \beta_3 = \frac{4\pi}{3ZR_0^3}\sqrt{\frac{B(E3)\uparrow}{\mathrm{e}^2}}, \quad (6)$$

with $R_0 = 1.2A^{1/3}$ fm. We note that the number of neutrons in ^{96}Zr nucleus is equal to one of the so-called "octupole magic" numbers 56 [27]. Low energy experiments indeed show that ^{96}Zr has a very large octupole collectivity corresponding to a large β_3 value, but a small β_2 value [28–30]. On the other hand, the ^{96}Ru nucleus has larger β_2, but shows no evidence of significant β_3. The latter is expected from the very large excitation energy for its 3_1^- state. In this analysis, we assume $\beta_{3,\mathrm{Ru}} = 0$. Note that the predictions from nuclear structure models [31] have large discrepancy from these data, therefore they are not used in this study.

	β_2	$E_{2_1^+}$ (MeV)	β_3	$E_{3_1^-}$ (MeV)
^{96}Ru	0.154	0.83	-	3.08
^{96}Zr	0.062	1.75	0.202,0.235,0.27	1.90

TABLE I. Values of β_2 deduced from the $B(E2;0_1^+\to 2_1^+)$ [32] and β_3 deduced from three $B(E3;0_1^+\to 3_1^-)$ [33] transition measurements via Eq. 6. The corresponding excitation energies are also provided. In general, larger excitation energy corresponds to smaller deformability for the nucleus.

To understand the hydrodynamic response to nuclear deformations and make predictions, we employ the multiphase transport model (AMPT) [34] as a proxy for hydrodynamics. This model is successful in describing collective flow data in small and large collision systems at RHIC and LHC [35–38] and has been used to study the β_n dependence of v_n [10, 11]. We use AMPT v2.26t5 in string-melting mode at $\sqrt{s_{\mathrm{NN}}}$ = 200 GeV, and a partonic cross section of 3.0 mb [36, 37], which gives a reasonable description of Au+Au and U+U v_2 data at RHIC [39, 40]. We simulate generic isobar ^{96}X+^{96}X collisions with $R_0 = 5.09$ fm and $a = 0.52$ fm. We performed a scan on β_2: $\beta_2 = 0, 0.05, 0.1, 0.15, 0.2$ and $\beta_3 = 0$, as well as a scan on β_3: $\beta_3 = 0, 0.05, 0.1, 0.15, 0.2$ and $\beta_2 = 0.06$. The ε_n are calculated from participating nucleons and v_n are calculated using two-particle correlation method with hadrons in $0.2 < p_{\mathrm{T}} < 2$ GeV and $|\eta| < 2$ [41].

The left panels of Fig. 1 show ratios of $\varepsilon_n(\beta_2,\beta_3)$ for given values of β_2 or β_3 to that for spherical nuclei. There are four different types of ratio considered, $\varepsilon_3(\beta_2,0)/\varepsilon_2(0,0)$, $\varepsilon_3(0,\beta_3)/\varepsilon_3(0,0)$, $\varepsilon_2(0,\beta_3)/\varepsilon_2(0,0)$, and $\varepsilon_3(\beta_2,0)/\varepsilon_3(0,0)$, i.e. we not only consider how the ε_n are affected by β_n but also the cross-correlation between ε_2 and β_3 or between ε_3 and β_2. Our study shows that the ε_n in Glauber model takes the following simplified version of Eq. 2 [12],

$$\varepsilon_2^2 = a_2' + b_2'\beta_2^2 + b_{2,3}'\beta_3^2,\ \ \varepsilon_3^2 = a_3' + b_3'\beta_3^2. \quad (7)$$

The ε_2 is strongly influenced by β_3 in the non-central collisions, reaching a maximum at $N_{\mathrm{part}} \sim 146$ corresponding to about 8% centrality. The right panels of Fig. 1 show ratios of v_n^2 with the same layout, which we found can be well parametrized by

$$v_2^2 = a_2 + b_2\beta_2^2 + b_{2,3}\beta_3^2,\ \ v_3^2 = a_3 + b_3\beta_3^2. \quad (8)$$

It is clear from Fig. 1 that the ratio of v_n in all cases is smaller than the ratio of ε_n for the same β_n. This observation implies that the hydrodynamic response for b' parameters are smaller than those for the a', i.e. $b_n/b_n' < a_n/a_n'$ and $b_{2,3}/b_{2,3}' < a_2/a_2'$. In other words, the contributions of v_n from nuclear deformation are more damped by hydrodynamic evolution than that from the eccentricity of the spherical nuclei. One possible explanation is that the nuclear deformation increases ε_n by adding more nucleons towards the edge of the overlap, leading to a weaker hydrodynamic response and less efficient conversion of ε_n to v_n.

With Eq. 7 in hand and using the values of β_n from Tab. I, we are ready to predict the v_n ratios between Ru+Ru and Zr+Zr collisions. Safely assuming $\beta_{3,\mathrm{Ru}} = 0$, these ratios are expected to scale like:

$$\frac{v_{2,\mathrm{Ru}}^2}{v_{2,\mathrm{Zr}}^2} \approx 1 + \frac{b_2}{a_2}(\beta_{2,\mathrm{Ru}}^2 - \beta_{2,\mathrm{Zr}}^2) - \frac{b_{2,3}}{a_2}\beta_{3,\mathrm{Zr}}^2, \quad (9)$$

$$\frac{v_{3,\mathrm{Ru}}^2}{v_{3,\mathrm{Zr}}^2} \approx 1 - \frac{b_3}{a_3}\beta_{3,\mathrm{Zr}}^2. \quad (10)$$

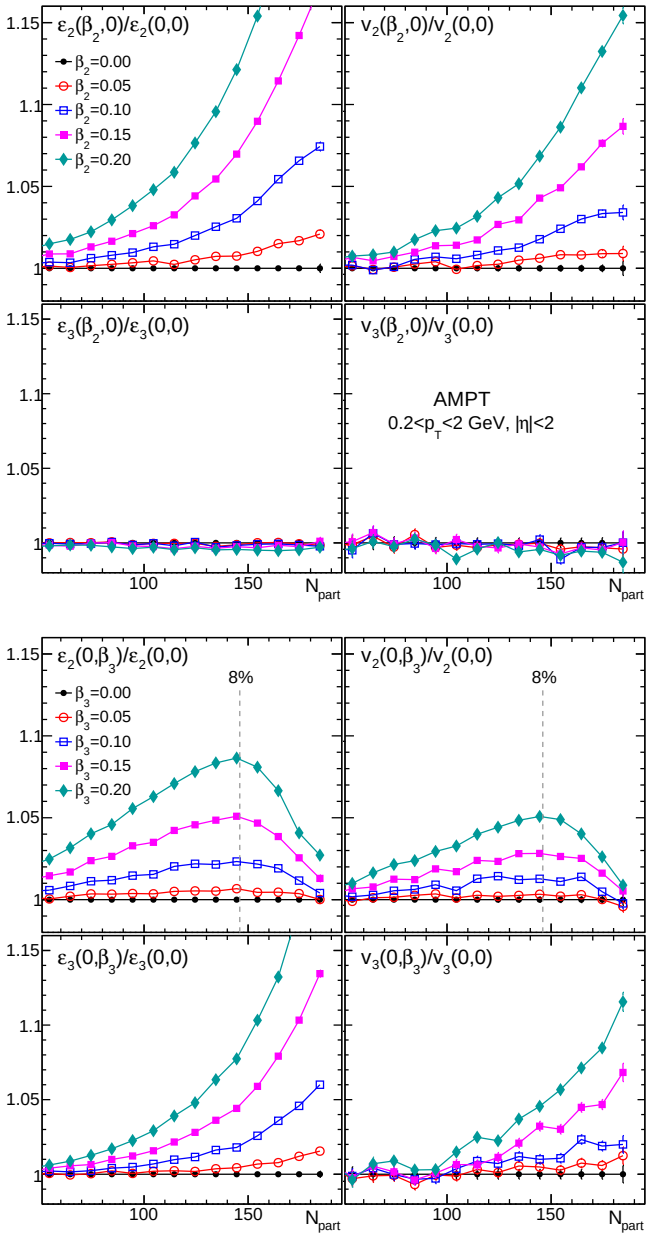

FIG. 1. The $N_{\rm part}$ dependence of ratios of ε_n (left column) or v_n (right column) relative to undeformed case with for $n = 2,3$ in generic ^{96}X+^{96}X collisions with different β_2 (top part) and β_3 (bottom part) values. The v_n are calculated in the AMPT models with hadrons in $|\eta| < 2$ and $0.2 < p_{\rm T} < 2$ GeV.

The coefficients b_n/a_n and $b_{2,3}/a_2$ can be calculated from Fig. 1 as a function of $N_{\rm part}$, which can then be used to predict $v_{n,\rm Ru}/v_{n,\rm Zr}$. Alternatively, $v_{n,\rm Ru}/v_{n,\rm Zr}$ can be obtained directly according to the β_n values in Tab. I,

$$\frac{v_{n,\rm Ru}}{v_{n,\rm Zr}} \approx \frac{v_n(\beta_{2,\rm Ru},0)}{v_n(\beta_{2,\rm Zr},0)} \times \frac{v_n(0,\beta_{3,\rm Ru})}{v_n(0,\beta_{3,\rm Zr})} = \frac{v_n(0.154,0)}{v_n(0.062,0)} \times \frac{v_n(0,0)}{v_n(0,0.2)} \ .$$

Since $\beta_{2,\rm Ru} \gg \beta_{2,\rm Zr}$ and value of $\beta_{3,\rm Zr}$ is large, the ratio $v_{2,\rm Ru}/v_{2,\rm Zr}$ is expected to contain a positive contribution from β_2 and a negative contribution from β_3. This is clearly demonstrated in the top panel of Fig. 2. The $\beta_{3,\rm Zr}$ has a small impact in the 0–1% centrality, but significantly reduces the v_2 ratio over the 1–40% centrality range, with the maximum reduction at around $N_{\rm part} \sim 146$ or 8% centrality. The influence of $\beta_{3,\rm Zr}$ also forces a much sharper decrease of the v_2 ratio in the centrality range of 0–5%, and leads to a non-monotonic centrality dependence. On the other hand, the predicted $v_{3,\rm Ru}/v_{3,\rm Zr}$ ratios in the bottom panel of Fig. 2 are independent of the β_2 of the two systems. This interesting interplay between β_2 and β_3, and the resulting features in the v_n ratio in the isobar collisions are salient and robust predictions that can be verified experimentally.

The STAR Collaboration has just released the $v_{n,\rm Ru}/v_{n,\rm Zr}$ data in several coarse centrality bins [25]; they are contrasted with our predictions in Fig. 2. The v_2 ratio data show non-monotonic centrality dependence similar in shape to our prediction that include effects of both β_2 and β_3, and such non-monotonicity was not predicted in previous studies that did not include the influence of β_3 [42, 43]. However our prediction is systematically lower than the STAR data by up to 2% in the mid-central and peripheral region. This residual difference could be due to the large neutron skin effect in ^{96}Zr [43], which was found to enhance $\varepsilon_{2,\rm Ru}/\varepsilon_{2,\rm Zr}$ with a shape and magnitude similar to this difference. Remarkably, our prediction of v_3 ratio agrees nearly perfectly with the STAR data over the entire centrality range when $\beta_{3,\rm Zr} = 0.2$ is used. This also raise a question whether the large β_3 value constrained by the isobar collisions could imply a large static octupole deformation in the ground state of ^{96}Zr, as implemented in our AMPT model simulation.

Next, we make predictions in the 0–1% most central collisions, where the influence of nuclear deformation is strongest, the contribution from β_3 to v_2 is small, and v_n ratios are expected to be described precisely by Eq. 5 with b_n/a_n as the only free parameters. The STAR data are not yet available in this region. Figure 3 shows the predicted ratio $v^2_{2,\rm Ru}/v^2_{2,\rm Zr}$ and $v^2_{3,\rm Ru}/v^2_{3,\rm Zr}$ as a function of $\beta^2_{2,\rm Ru}$ and $\beta^2_{3,\rm Zr}$, respectively. The predictions follow strictly a linear dependence on β^2_n. Assuming the $\beta_{2,\rm Ru} = 0.154$ and $\beta_{2,\rm Zr} = 0.062$ from Table I, we predicts a $v^2_{2,\rm Ru}/v^2_{2,\rm Zr} \approx 1.16$, corresponding to $v_{2,\rm Ru}/v_{2,\rm Zr} \approx 1.08$. On the other hand, the three octupole deformation values from nuclear structure measurements, $\beta_{3,\rm Zr} = 0.202, 0.235, 0.27$, would predict $v^2_{3,\rm Zr}/v^2_{3,\rm Ru} = 1.24, 1.33, 1.44$ as indicated by the solid arrows in Fig. 3, or equivalently $v_{3,\rm Ru}/v_{3,\rm Zr} = 0.90, 0.87, 0.83$. The latter two cases, $\beta_{3,\rm Zr} = 0.235$ and 0.27, are clearly ruled out by the data-theory comparison of the v_3 ratio in the bottom panel of Fig. 2. These two $\beta_{3,\rm Zr}$ values would also lead to further reduction of the $v_{2,\rm Ru}/v_{2,\rm Zr}$ ratio (indicated by the open circles) in the top panel of Fig. 2. This additional reduction amount to $0.235^2/0.2^2 - 1 = 38\%$ or

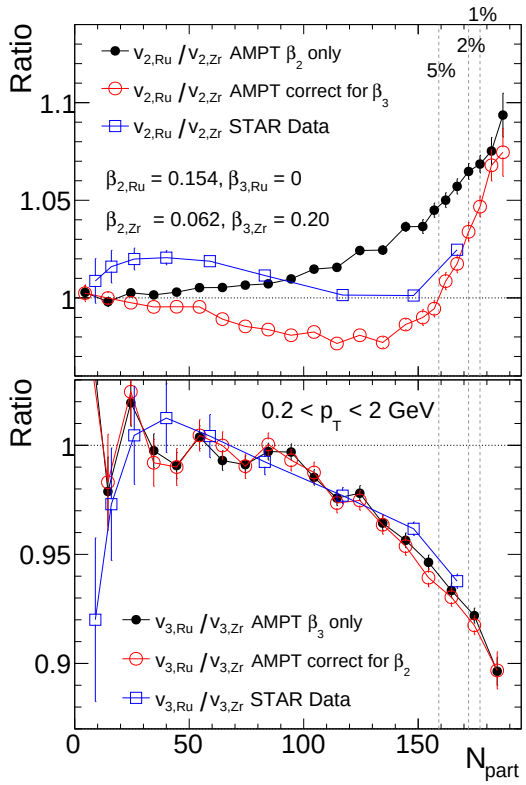

FIG. 2. Predicted ratios of v_2 (top) and v_3 (top) between Ru+Ru and Zr+Zr collisions from the AMPT model based on the β_2 and β_3 values for Ru and Zr from Table I. They are compared with the STAR data from Ref. [25].

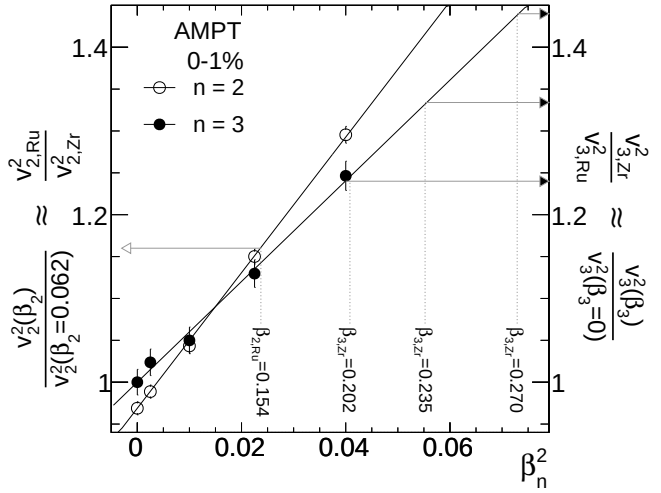

FIG. 3. Predicted ratio of $v_{2,\mathrm{Ru}}^2/v_{2,\mathrm{Zr}}^2$ as a function of $\beta_{2,\mathrm{Ru}}^2$ assuming $\beta_{2,\mathrm{Zr}}$ = 0.062 (open symbols), and ratio of $v_{3,\mathrm{Zr}}^2/v_{3,\mathrm{Ru}}^2$ as a function of $\beta_{3,\mathrm{Zr}}^2$ assuming $\beta_{3,\mathrm{Ru}}$ = 0 (filled symbols) from the AMPT model for the 0–1% centrality. The arrows indicate the corresponding ratios for $\beta_{2,\mathrm{Ru}}$ = 0.154 (left pointing) and $\beta_{3,\mathrm{Zr}}$ = 0.202, 0.235 and 0.27 from Table I (right pointing).

$0.27^2/0.2^2 - 1 = 82\%$ of the difference between the two AMPT predictions, which will make both the shape and the magnitude of the $v_{2,\mathrm{Ru}}/v_{2,\mathrm{Zr}}$ incompatible with the experimental data even after including the predicted neutron skin effects [43]. Therefore, for the first time, the isobar collisions show clear potential for providing new constraints on nuclear deformation parameters that can complement those from nuclear structure spectroscopy in testing state-of-the-art nuclear structure models. In order to pin down the interplay between β_2 and β_3 more quantitatively, however, STAR measurement [25] should be extended to finer centrality bins, especially in the 0–5% range where the v_n ratios are still changing very rapidly.

A few homeworks are required in order to accomplish a precision determination of nuclear deformations using heavy ion collisions. First and most importantly, we need to understand the connection of the β_n given by nuclear structure method Eq. 6 and β_n in heavy ion collisions via Eq. 1. The former measures the charge distribution at the timescale of 10^{-21}s, while the heavy ion collisions cares only about the mass distribution at a much shorter time of 10^{-24}s, which is also strongly Lorentz contracted unlike in the low-energy experiments. For example, changing the R_0 value alone in Eq. 6 would directly change the value of extracted β_n, but changing the R_0 in Eq. 1 has little impact on the hydrodynamic response to β_n. From the modeling side of the heavy ion collisions, we need to pin down the hydrodynamic response of v_n to the deformation contribution to the eccentricity, which is clearly different from the hydrodynamic response of v_n to the baseline eccentricity for spherical nuclei (see Fig. 1). Further hydrodynamic models studies are required to quantify the systematic uncertainties, in particular the ratio a_n/b_n. Nevertheless, the STAR results and our study demonstrate that heavy ion collisions can serve as a new tool for imaging the shape of the atomic nuclei and possibly other features of their nuclear structure. This provides good arguments for an extended system scan of different isobaric systems for precision measurement of interesting nuclear structure effects and complement the low energy methods [11, 12].

In summary, recent STAR measurement of v_2 and v_3 show significant differences between ^{96}Zr+^{96}Zr and ^{96}Ru+^{96}Ru collisions. Using a transport simulation, we show that these differences can be naturally explained from the large quadrupole deformation β_2 of ^{96}Ru and large octupole deformation β_3 of ^{96}Zr. Our calculations quantitively describe the $v_{3,\mathrm{Ru}}/v_{3,\mathrm{Zr}}$ by assuming $\beta_{3,\mathrm{Zr}}$ = 0.2 from one nuclear structure measurement. However, the presence of $\beta_{3,\mathrm{Zr}}$ was found to significantly enhance the $v_{2,\mathrm{Zr}}$ and led to a non-monotonic centrality dependence of $v_{2,\mathrm{Ru}}/v_{2,\mathrm{Zr}}$ as observed in the data. Additional physics such as neutron skin differences are also required to quantitively describe the v_2 ratio. Our analysis demonstrates that isobaric heavy ion collisions can

be used as a precision tool to image the shape and radial structures of the nuclei. We hope this can be done in the existing high-energy collider facilities in the near future.

Acknowledgements: We thank Yu Hu for providing the STAR data. We thank Giuliano Giacalone for proof reading the draft and his valuable suggestions. We acknowledge Somadutta Bhatta for discussions during the development of this work. This work is supported by DOE DEFG0287ER40331.

* Correspond to jiangyong.jia@stonybrook.edu

[1] Kris Heyde and John L. Wood, "Shape coexistence in atomic nuclei," Rev. Mod. Phys. **83**, 1467–1521 (2011).
[2] K. Heyde and J. L. Wood, "Nuclear shapes: from earliest ideas to multiple shape coexisting structures," Phys. Scripta **91**, 083008 (2016).
[3] Ulrich W. Heinz and Anthony Kuhlman, "Anisotropic flow and jet quenching in ultrarelativistic U + U collisions," Phys. Rev. Lett. **94**, 132301 (2005), arXiv:nucl-th/0411054.
[4] Peter Filip, Richard Lednicky, Hiroshi Masui, and Nu Xu, "Initial eccentricity in deformed ^{197}Au + ^{197}Au and ^{238}U + ^{238}U collisions at $\sqrt{s_{\rm NN}}$ = 200 GeV at the BNL Relativistic Heavy Ion Collider," Phys. Rev. C **80**, 054903 (2009).
[5] Q. Y. Shou, Y. G. Ma, P. Sorensen, A. H. Tang, F. Videbæk, and H. Wang, "Parameterization of Deformed Nuclei for Glauber Modeling in Relativistic Heavy Ion Collisions," Phys. Lett. B **749**, 215–220 (2015), arXiv:1409.8375 [nucl-th].
[6] Andy Goldschmidt, Zhi Qiu, Chun Shen, and Ulrich Heinz, "Collision geometry and flow in uranium + uranium collisions," Phys. Rev. C **92**, 044903 (2015), arXiv:1507.03910 [nucl-th].
[7] Giuliano Giacalone, Jacquelyn Noronha-Hostler, Matthew Luzum, and Jean-Yves Ollitrault, "Hydrodynamic predictions for 5.44 TeV Xe+Xe collisions," Phys. Rev. C **97**, 034904 (2018), arXiv:1711.08499 [nucl-th].
[8] Giuliano Giacalone, "Elliptic flow fluctuations in central collisions of spherical and deformed nuclei," Phys. Rev. C **99**, 024910 (2019), arXiv:1811.03959 [nucl-th].
[9] Giuliano Giacalone, Jiangyong Jia, and Vittorio Somà, "Accessing the shape of atomic nuclei with relativistic collisions of isobars," (2021), arXiv:2102.08158 [nucl-th].
[10] Giuliano Giacalone, Jiangyong Jia, and Chunjian Zhang, "The impact of nuclear deformation on relativistic heavy-ion collisions: assessing consistency in nuclear physics across energy scales," (2021), arXiv:2105.01638 [nucl-th].
[11] Jiangyong Jia, Shengli Huang, and Chunjian Zhang, "Constraining nuclear quadrupole deformation from correlation of elliptic flow and transverse momentum in nuclear collisions," (2021), arXiv:2105.05713 [nucl-th].
[12] Jiangyong Jia, "Shape of atomic nuclei in heavy ion collisions," (2021), arXiv:2106.08768 [nucl-th].
[13] Benjamin Bally, Michael Bender, Giuliano Giacalone, and Vittorio Somà, "Evidence of the triaxial structure of ^{129}Xe at the Large Hadron Collider," (2021), arXiv:2108.09578 [nucl-th].
[14] L. Adamczyk *et al.* (STAR), "Azimuthal anisotropy in U+U and Au+Au collisions at RHIC," Phys. Rev. Lett. **115**, 222301 (2015), arXiv:1505.07812 [nucl-ex].
[15] S. Acharya *et al.* (ALICE), "Anisotropic flow in Xe-Xe collisions at $\sqrt{s_{\rm NN}}$ = **5.44** TeV," Phys. Lett. B **784**, 82–95 (2018), arXiv:1805.01832 [nucl-ex].
[16] Albert M Sirunyan *et al.* (CMS), "Charged-particle angular correlations in XeXe collisions at $\sqrt{s_{\rm NN}}$ = 5.44 TeV," Phys. Rev. C **100**, 044902 (2019), arXiv:1901.07997 [hep-ex].
[17] Georges Aad *et al.* (ATLAS), "Measurement of the azimuthal anisotropy of charged-particle production in Xe+Xe collisions at $\sqrt{s_{\rm NN}}$ = 5.44 TeV with the ATLAS detector," Phys. Rev. C **101**, 024906 (2020), arXiv:1911.04812 [nucl-ex].
[18] Jiangyong Jia, "Nuclear deformation effects via Au+Au and U+U collisions from STAR," Contribution to the VI$^{\rm th}$ International Conference on the Initial Stages of High-Energy Nuclear Collisions, January 2021, https://indico.cern.ch/event/854124/contributions/4135480/.
[19] Including other internal shape degrees of freedom, such as triaxiality, does not affect the two-particle observables ε_n^2 and v_n^2 [12].
[20] Wit Busza, Krishna Rajagopal, and Wilke van der Schee, "Heavy Ion Collisions: The Big Picture, and the Big Questions," Ann. Rev. Nucl. Part. Sci. **68**, 339–376 (2018), arXiv:1802.04801 [hep-ph].
[21] Ulrich W. Heinz, "Towards the Little Bang Standard Model," J. Phys. Conf. Ser. **455**, 012044 (2013), arXiv:1304.3634 [nucl-th].
[22] H. Niemi, K. J. Eskola, and R. Paatelainen, "Event-by-event fluctuations in a perturbative QCD + saturation + hydrodynamics model: Determining QCD matter shear viscosity in ultrarelativistic heavy-ion collisions," Phys. Rev. C **93**, 024907 (2016), arXiv:1505.02677 [hep-ph].
[23] Björn Schenke, Chun Shen, and Derek Teaney, "Transverse momentum fluctuations and their correlation with elliptic flow in nuclear collision," Phys. Rev. C **102**, 034905 (2020), arXiv:2004.00690 [nucl-th].
[24] Jiangyong Jia, "Probing triaxial deformation of atomic nuclei in high-energy heavy ion collisions," (2021), arXiv:2109.00604 [nucl-th].
[25] Mohamed Abdallah *et al.* (STAR), "Search for the Chiral Magnetic Effect with Isobar Collisions at $\sqrt{s_{\rm NN}}$ = 200 GeV by the STAR Collaboration at RHIC," (2021), arXiv:2109.00131 [nucl-ex].
[26] Aage Bohr and Ben R Mottelson, eds., *Nuclear Structure II, Page 348* (World Scientific, 1998).
[27] P. A. Butler and W. Nazarewicz, "Intrinsic reflection asymmetry in atomic nuclei," Rev. Mod. Phys. **68**, 349–421 (1996).
[28] M. M. Stautberg, R. R. Johnson, J. J. Kraushaar, and B. W. Ridley, "The 96 Zr(p, p') and 96 Zr(p, d) reaction at 19.4 MeV," Nucl. Phys. A **104**, 67–80 (1967).
[29] H. Mach, S. Cwiok, W. Nazarewicz, B. Fogelberg, M. Moszynski, J. Winger, and R. L. Gill, "Strong octupole and dipole collectivity in Zr-96: Indication for octupole instability in the A=100 mass region," Phys. Rev. C **42**, R811–R814 (1990).
[30] D. Hofer *et al.*, "Direct and multiple excitations in 96 Zr from inelastic-scattering experiments," Nucl. Phys. A **551**, 173–209 (1993).
[31] P. Möller, A. J. Sierk, T. Ichikawa, and H. Sagawa,

"Nuclear ground-state masses and deformations: FRDM(2012)," Atom. Data Nucl. Data Tabl. **109-110**, 1–204 (2016), arXiv:1508.06294 [nucl-th].

[32] B. Pritychenko, M. Birch, B. Singh, and M. Horoi, "Tables of E2 Transition Probabilities from the first 2^+ States in Even-Even Nuclei," Atom. Data Nucl. Data Tabl. **107**, 1–139 (2016), [Erratum: Atom.Data Nucl.Data Tabl. 114, 371–374 (2017)], arXiv:1312.5975 [nucl-th].

[33] T Kibédi and R. H Spear, "reduced electric-octupole transition probabilities, $B(E3;0_1^+ \rightarrow 3_1^-)$ an update," Atom. Data Nucl. Data Tabl. **80**, 35–82 (2002).

[34] Zi-Wei Lin, Che Ming Ko, Bao-An Li, Bin Zhang, and Subrata Pal, "A Multi-phase transport model for relativistic heavy ion collisions," Phys. Rev. **C72**, 064901 (2005), arXiv:nucl-th/0411110 [nucl-th].

[35] A. Adare *et al.* (PHENIX), "Measurements of directed, elliptic, and triangular flow in Cu+Au collisions at $\sqrt{s_{\rm NN}}$ = 200 GeV," Phys. Rev. **C94**, 054910 (2016), arXiv:1509.07784 [nucl-ex].

[36] Guo-Liang Ma and Adam Bzdak, "Long-range azimuthal correlations in protonproton and protonnucleus collisions from the incoherent scattering of partons," Phys. Lett. **B739**, 209–213 (2014), arXiv:1404.4129 [hep-ph].

[37] Adam Bzdak and Guo-Liang Ma, "Elliptic and triangular flow in p+Pb and peripheral Pb+Pb collisions from parton scatterings," Phys. Rev. Lett. **113**, 252301 (2014), arXiv:1406.2804 [hep-ph].

[38] Mao-Wu Nie, Peng Huo, Jiangyong Jia, and Guo-Liang Ma, "Multiparticle azimuthal cumulants in p+Pb collisions from a multiphase transport model," Phys. Rev. **C98**, 034903 (2018), arXiv:1802.00374 [hep-ph].

[39] Jun Xu and Che Ming Ko, "Triangular flow in heavy ion collisions in a multiphase transport model," Phys. Rev. C **84**, 014903 (2011), arXiv:1103.5187 [nucl-th].

[40] Mohamed Abdallah *et al.* (STAR), "Azimuthal anisotropy measurements of strange and multistrange hadrons in $U+U$ collisions at $\sqrt{s_{NN}}$ =193 GeV at the BNL Relativistic Heavy Ion Collider," Phys. Rev. C **103**, 064907 (2021), arXiv:2103.09451 [nucl-ex].

[41] Georges Aad *et al.* (ATLAS), "Measurement of the azimuthal anisotropy for charged particle production in $\sqrt{s_{\rm NN}}$ = 2.76 TeV lead-lead collisions with the ATLAS detector," Phys. Rev. **C86**, 014907 (2012), arXiv:1203.3087 [hep-ex].

[42] Wei-Tian Deng, Xu-Guang Huang, Guo-Liang Ma, and Gang Wang, "Test the chiral magnetic effect with isobaric collisions," Phys. Rev. C **94**, 041901 (2016), arXiv:1607.04697 [nucl-th].

[43] Hao-jie Xu, Hanlin Li, Xiaobao Wang, Caiwan Shen, and Fuqiang Wang, "Determine the neutron skin type by relativistic isobaric collisions," Phys. Lett. B **819**, 136453 (2021), arXiv:2103.05595 [nucl-th].